



## On modeling chronic detachment of periphyton in artificial rough, open channel flow

Myriam Graba<sup>a,b,c,\*</sup>, Ahmed Kettab<sup>a</sup>, Sabine Sauvage<sup>b,c</sup>, José Miguel Sanchez-Pérez<sup>b,c</sup>

<sup>a</sup>Ecole Nationale Polytechnique/Laboratoire des Sciences de l'Eau, 10 Avenue Hassen Badi, El Harrach, Alger.,  
Algerie

Tel. +213 (0) 7 70 51 92 38/+33 (0) 6 62 35 38 71; Fax: +213 (0) 34 21 51 05; email: myriam.graba@univ-tlse3.fr

<sup>b</sup>Université de Toulouse; INP, UPS; EcoLab (Laboratoire d'Ecologie Fonctionnelle et Environnement),

Avenue de l'Agrobiopôle, 31326, Castanet Tolosane, France

<sup>c</sup>CNRS; EcoLab, 31326, Castanet, Tolosan, France

Received 13 April 2011; Accepted 15 January 2012

---

### ABSTRACT

Periphyton communities, which are native to river beds, serve as a functional indicator of river health but remain one of the least-studied communities despite the significant increase in the examination of aquatic microbial communities in recent years. In this study, we tested the relevance of three formulations of the chronic detachment term in a simple model for the biomass dynamics of periphyton. Numerical simulations of the periphyton biomass dynamics were performed by using three different descriptors for the flow conditions: the discharge  $Q$ , the friction velocity  $u_{*r}$ , and the roughness Reynolds number  $k^+ = u_* k_s / \nu$  (where  $\nu$  is water kinetic viscosity and  $k_s$  is the Nikuradse equivalent sand roughness). Comparisons of numerical simulation results with experimental data from literature revealed chronic detachment to be better simulated by taking the roughness Reynolds number as the external variable of detachment. These results support the idea that transport phenomena that occur in the near-bed layer, e.g. chronic detachment of periphyton matter or vertical transport of nutrients and pollutants in submerged aquatic canopies, are not related to a single turbulence descriptor such as the friction velocity  $u_*$ . Its description requires at least two descriptors, here the friction velocity  $u_*$  and the Nikuradse equivalent sand roughness  $k_s$ , which depend on the initial form and dimensions of the colonized substratum, and its changes owing to the thickness, resistance, and composition of the epilithic matter.

*Keywords:* Periphyton; Open-channel flow; Roughness; Friction velocity; Biomass dynamics; Turbulent boundary layer

---

### 1. Introduction

A number of recent studies show that the near-bed hydraulic habitat influences many biological processes which determine the function of the benthic communities in streams [1–3]. Among these communities,

periphyton is arguably one of the most important components of stream ecosystems. Periphyton, which grows on the river bed, is composed mainly of algae, bacteria, and fungi, is often the dominant source of energy for higher trophic levels [4–8] and is the habitat for other organisms. Rivers characterized by long periods of hydrological stability interrupted by floods and droughts enhance growth and proliferation of

---

\*Corresponding author.

periphyton and filamentous algae [9]. Excessive periphyton causes many problems such as degradation of ecosystem structure [2] and esthetic values [9], degradation of water quality (e.g. fluctuations in dissolved oxygen and pH) [10], and clogging of management structures [11]. Most severe cases occur under high nutrient loadings, which may originate from areas of nutrient-rich rocks, intensive agricultural development, and/or nutrient-rich waste discharges [2]. Thus, for better management of fluvial ecosystems dominated by fixed biomass in the near-bed region, the periphyton dynamics should be considered in numerical modeling of biogeochemical transfer.

The short-term temporal dynamics of the periphyton biomass results from the balance between the processes of accretion (immigration/colonization and proliferation of cells) and of loss (death and/or emigration of cells also called chronic detachment). The state of the knowledge relative to these dynamics was conceptualized by the work of Biggs [2] that represents these dynamics by a theoretical curve in two phases (Fig. 1). Accrual through immigration/colonization and growth dominates early in the “accrual phase”, but then there is a shift to dominance of loss processes through death, emigration, sloughing, and grazing later in the “loss phase” [2].

Flow is an important factor involved in the periphyton dynamics process, it has a stimulatory effect on algal metabolism and nutrient uptakes [9,12–14] and therefore on growth process. Also, the drag forces and the shear stress exerted by the flow of water over the periphyton community influence colonization and detachment process by affecting their ability to hold station or to attach the river bed [15–18].

Conversely, periphyton can modify local hydrodynamic characteristics such as the Nikuradse equivalent sand roughness  $k_s$ , which estimates the bed roughness height, the friction velocity  $u_*$ , which measures the

drag of the flow at the bottom [19], and then the roughness Reynolds number  $k^+ = u_*k_s/\nu$  (where  $\nu$  is water kinetic viscosity), a descriptor of the hydraulic roughness of the flow. Reiter [20,21] and Nikora et al. [22,23] found that friction velocity  $u_*$  increased with the growth of the periphyton, and hence increased the bed roughness. In contrast, Biggs and Hickey [24] observed that periphyton decreased the bed roughness.

The contradiction in conclusions of these earlier studies demonstrates the complexity of flow–periphyton interactions and has motivated further research in the past decade [14,25–29]. These latter studies show that the presence of the periphyton induces a clear variation in turbulence intensity and Reynolds shear stress in the benthic zone (interfacial region between the periphyton and the flow). Hence, the representation of the biomass dynamics of periphyton requires local parameters associated with the turbulent processes (such as the Reynolds number) instead of vertically integrated quantities such as flow discharge (Uehlinger et al. [16]) or mean longitudinal velocity (Saravia et al. [15], Horner and Welch [30] and Horner et al. [31]).

Thus, to improve periphyton biomass dynamics modeling, and particularly modeling the chronic detachment which is a process of continual biomass loss (emigration or export) generated by the drag exerted by the flow on cells near the substratum surface [32], Fothi [27] suggested replacing the flow discharge  $Q$  with the roughness Reynolds number  $k^+$  in the model of Uehlinger et al. [16]. However, Labiod et al. [28] adopted an intermediate step by taking the friction velocity  $u_*$  as external physical parameter for the chronic detachment. First evaluations of these models [27,28] gave better results than the early model of Uehlinger et al. [16]. Recently, we tested [33] these two formulations of the chronic detachment

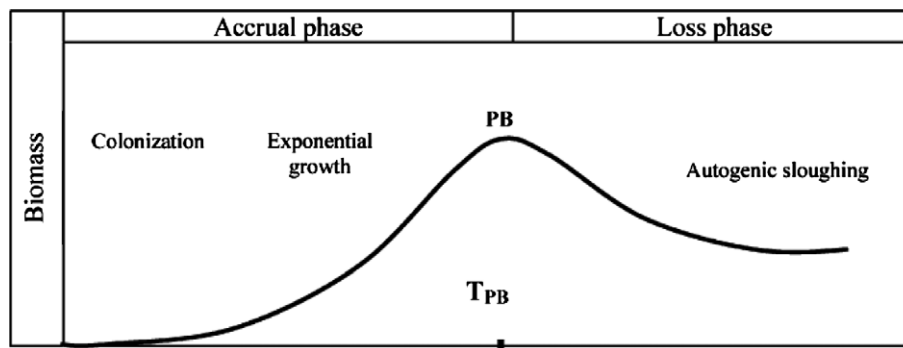


Fig. 1. An idealized benthic algal accrual curve with different phases shown. PB (peak of biomass) is the maximum accrual cycle biomass and TPB is the time to PB from commencement of colonization [2].

through numerical simulations and compared them with the data from laboratory experiments obtained in open-channel flow. We found that chronic detachment seems to be best simulated by taking the roughness Reynolds number as the external physical variable for forcing the chronic detachment. However, additional testing and experimental data are required to confirm or contradict the relevance of  $k^+$  or  $u_*$  alone. Hence, in the present study, data of biomass (Chl-a) and hydrodynamics ( $Q$ ,  $u_*$  and  $k_s$ ) measurements presented in Labiod et al. [28] were taken back and used in new simulations and confrontations of the relevance of the friction velocity  $u_*$  or the roughness Reynolds number  $k^+$  as the external physical variable for forcing the chronic detachment process.

## 2. Method

### 2.1. Model development

Among the models developed to reproduce the dynamics of periphyton [34–36,38], that of Uehlinger et al. [16] has been the most frequently used for natural or artificial river flows [17,18,27,28]. The level of complexity of this model was investigated by Boulétreau et al. [18], using the Akaike Information Criterion (AIC) to determine the minimum adequate parameter set required to describe the biomass dynamics. They found that in 9 of the 11 cases studied, the best model was one that described an equilibrium between phototrophic growth and discharge-dependent chronic loss (chronic detachment), and that ignored light, temperature, nutrient influences, and catastrophic or/and autogenic detachment terms. This simplified model reads:

$$\frac{dB}{dt} = G - D = \underbrace{\mu_{\max} B}_{G1} \underbrace{\frac{1}{1 + k_{\text{inv}} B}}_{G2} - \underbrace{C_{\text{det}} QB}_D \quad (1)$$

where  $B$  ( $\text{g}/\text{m}^2$ ) is the periphyton biomass,  $t$  (days) is the time,  $\mu_{\max}$  ( $\text{days}^{-1}$ ) is the maximum specific growth rate at the reference temperature  $20^\circ\text{C}$ ,  $k_{\text{inv}}$  ( $\text{g}^{-1} \text{m}^2$ ) is the inverse half-saturation constant for biomass,  $C_{\text{det}}$  ( $\text{s}/\text{m}^3 \text{days}^{-1}$ ) is an empirical detachment coefficient, and  $Q$  ( $\text{m}^3/\text{s}$ ) is the flow discharge. In this simplified model,  $G$  is a growth function formed by the linear term  $G1$ , which describes the exponential increase in biomass, and the term  $G2$ , which describes the effect of density limitation and characterizes the biomass limitation of the growth rate. It accounts for the phenomenon of biomass growth rate decreasing with increasing periphyton mat thickness, due to limitations in light and nutrient concentration in the inner layers of the periphyton.  $D$  is the chronic detachment

function, which is controlled here by the flow discharge  $Q$  and the biomass  $B$  and does not take into account grazing or catastrophic loss of biomass due to bed movement. These two latter processes were assumed to be negligible or nonexistent in laboratory experiments [28,33].

### 2.2. Chronic detachment functions formulation

As discussed previously, the detachment equation, with a global hydrodynamic parameter  $Q$  ( $\text{m}^3/\text{s}$ ) [16], cannot realistically describe a phenomenon such as the detachment that occurs on the bed where the periphyton grows. However, the function of chronic detachment can be described in a more pertinent equation, by taking as external physical variables local hydrodynamic characteristics, such as the friction velocity  $u_*$  or the roughness Reynolds number  $k^+ = u_* k_s / \nu$ , where  $\nu$  is water kinetic viscosity and  $k_s$  is the Nikuradse equivalent sand roughness.

Thus, three models can be inferred from Eq. (1), with three formulations ( $D_1$ ,  $D_2$ , and  $D_3$ ) for the chronic detachment function  $D$  as follows:

$$D_1 = C_{\text{det}} QB \quad (2)$$

$$D_2 = C'_{\text{det}} u_* B \quad (3)$$

$$D_3 = C''_{\text{det}} k^+ B \quad (4)$$

where  $Q$  ( $\text{m}^3/\text{s}$ ) is the discharge flow,  $u_*$  ( $\text{m}/\text{s}$ ) is the friction velocity,  $k^+$  ( $=u_* k_s / \nu$ ) is the dimensionless roughness Reynolds number, and  $C_{\text{det}}$  ( $\text{s}/\text{m}^3 \text{days}^{-1}$ ),  $C'_{\text{det}}$  ( $\text{s}/\text{m} \text{days}^{-1}$ ), and  $C''_{\text{det}}$  ( $\text{days}^{-1}$ ) are detachment coefficients that represent respectively the daily detached biomass per surface unit ( $\text{mg}/\text{m}^2$ ) for each unity of discharge, friction velocity, and roughness Reynolds number.

According to the considerations above and with the knowledge that the factors of light, temperature, nutrient availability, and grazers were controlled in the experimental flumes, the models that we tested all read:

$$\frac{dB}{dt} = G - D \quad (5)$$

with the growth function  $G = \mu_{\max} B \frac{1}{1 + k_{\text{inv}} B}$  and three equations ( $D_1$ ,  $D_2$ , and  $D_3$ ) for the chronic detachment function  $D$ .

### 2.3. Numerical model description

The differential Eq. (5) for each of the three chronic detachment equations ( $D_1$ ,  $D_2$ , and  $D_3$ ) was solved

numerically by coding the fourth-order Runge–Kutta method in Fortran 90. We noted that in this equation inferred from the model of Uehlinger et al. [16], colonization is not considered. We therefore decided to describe the colonization process by an initial condition for the biomass, adopting a numerical parameterization [39,40] to determine the value of the initial epilithic biomass denoted  $B_{\text{init}}$ . Preliminary tests demonstrated that a time step fixed at 3 h was a good condition to reduce errors caused by numerical integration.

### 3. Application

The numerical models with the three formulations for the chronic detachment parameter have been applied to the results of an experimental study conducted by Labiod et al. [28]. This study measured the periphyton density evolution (in time) using Chl-a concentration by surface unity ( $\text{g}/\text{m}^2$ ) and the evolution of the local flow descriptors ( $u_*$  and  $k_s$ ) during periphyton growth in three experiments (Run1, Run2, and Run3). The experiments were conducted in an open-channel flow with rough bed “PVC rods (diameter 10 mm) arranged side by side and perpendicular to the side walls of the channel, representing 2-D roughness” [28]. Discharge was maintained constant during the experiments (7.51/s in Run1, 121/s in Run2, and 191/s in Run3 [28]) and light, temperature, and concentrations of nutrients were stable and similar in the flume for the three experimental runs. The velocity components were measured using a Laser Doppler Anemometer (LDA). Values of  $u_*$  have been calculated using the root mean square (RMS) values of the velocity fluctuations in the longitudinal and vertical directions. While values of  $k_s$  were deduced from a classical least-square fitting of longitudinal velocity profiles in the inner region that satisfy a log low distribution (see Labiod et al. [28] for more details on procedures). Then, values of  $k^+$  have been calculated from the formulation  $k^+ = u_* k_s / \nu$ , where  $\nu$  is water kinetic viscosity,  $u_*$  is the friction velocity, and  $k_s$  is the Nikuradse equivalent sand roughness.

For our numerical simulations, values of the input data (friction velocity  $u_*$  and roughness Reynolds number  $k^+$ ) at each time step (1 day) were obtained by linear interpolation of the three experimental data-sets presented in Labiod et al. [28] and are reproduced in Table 1.

To calibrate the models for each run, we started by adjusting the values of the maximum specific growth  $\mu_{\text{max}}$  ( $\text{days}^{-1}$ ), the inverse half-saturation constant  $k_{\text{inv}}$

Table 1

Evolution of the near-bed parameters on the flume during the three runs [27]

| Run  | Day | $u_*$ ( $\text{m s}^{-1}$ ) | $k_s$ (mm) | $k^+$  |
|------|-----|-----------------------------|------------|--------|
| Run1 | 0   | 0.0130                      | 0.15       | 1.95   |
|      | 8   | 0.0160                      | 1.56       | 24.96  |
|      | 12  | 0.0165                      | 2.73       | 45.04  |
|      | 19  | 0.0172                      | 3.26       | 56.07  |
|      | 26  | 0.0210                      | 5.71       | 119.91 |
| Run2 | 0   | 0.0198                      | 1.77       | 35.04  |
|      | 6   | 0.0192                      | 1.82       | 34.94  |
|      | 12  | 0.0190                      | 1.58       | 30.02  |
|      | 21  | 0.0288                      | 8.33       | 239.90 |
|      | 26  | 0.0300                      | 8.00       | 240.00 |
| Run3 | 0   | 0.0220                      | 1.45       | 31.90  |
|      | 8   | 0.0247                      | 2.23       | 55.08  |
|      | 13  | 0.0272                      | 2.39       | 65.01  |
|      | 27  | 0.0299                      | 4.68       | 139.93 |

Table 2

Numerical and empirical parameter values used for biomass (Chl-a,  $\text{mg}/\text{m}^2$ ) growth simulations

| Parameters  | Run1      | Run2      | Run3      |
|---|-----------|-----------|-----------|
| $B_{\text{init}}$ ( $\text{g}/\text{m}^2$ )                 | $10^{-3}$ | $10^{-2}$ | $10^{-1}$ |
| $\mu_{\text{max}}$ ( $\text{days}^{-1}$ )                   | 1.1       | 1.1       | 0.7       |
| $k_{\text{inv}}$ ( $\text{g}^{-1} \text{m}^2$ )             | 0.05      | 0.07      | 0.03      |
| $C_{\text{det}}$ ( $\text{s}/\text{m}^3 \text{days}^{-1}$ ) | 17        | 5         | 7         |
| $C'_{\text{det}}$ ( $\text{s}/\text{m} \text{days}^{-1}$ )  | 8         | 7         | 6         |
| $C''_{\text{det}}$ ( $\text{days}^{-1}$ )                   | 0.0024    | 0.001     | 0.002     |

( $\text{g}^{-1} \text{m}^2$ ), and the initial biomass  $B_{\text{init}}$  in the range of values reported in the literature from field, laboratory, and modeling studies for phytoplanktonic and benthic algae [16,18,41,42], this, to have the best correlation between the measurements and the simulations on the complete simulation period. Then, for each run, and for each of the three chronic detachment formulations, the parameters  $C_{\text{det}}$ ,  $C'_{\text{det}}$ , and  $C''_{\text{det}}$  were chosen to have also the best fit between the simulated and the measured values (Table 2).

## 4. Results and discussion

### 4.1. Model testing and evaluation

The results of the simulations with the three detachment formulations (D1, D2, and D3) were compared with the three experimental data-sets. In order to determine the empirical and numerical parameters of the simulation, we looked at the parameters that

gave the best simulations (using the coefficient of correlation  $R^2$ ) of the changes in Chl-a for each of the three runs and of the three formulations of the chronic detachment term. The values retained for the final simulations (Run1, Run2, and Run3) and for the comparisons are summarized in Table 2. These values, which are dependent on the specific conditions of the experiment in terms of nutrient availability, light incidence, temperature, turbulence intensity, shear stress, and algal composition, cannot be generalized to other conditions of growth of periphyton.

Calibration of initial biomass gives different values for each of the three runs (see Table 2). Thus, as we adopted a numerical parameterization to describe the colonization process by an initial condition (see Section 2.2. Numerical model description),  $B_{init}$  represents also the colonization process. So, while knowing that the values 7.51/s in Run1, 121/s in Run2, and 191/s in Run3 [28], the values of the initial biomass found for each run ( $B_{init}=10^{-3} \text{ g m}^{-2}$  in Run1,  $B_{init}=10^{-2} \text{ g m}^{-2}$  in Run2 and  $B_{init}=10^{-1} \text{ g m}^{-2}$  in Run3) are in accordance with the recent results of Godillot et al. [25] and Moulin et al. [29], who observed “that the higher flows regimes delayed the colonization process”. For the chronic detachment that is the focus of this study, periphyton does not have the same morphology and tolerance for shear stress, and the magnitude of shear stress which causes

detachment of algae differs significantly between species, particularly taxa growing in fast flow and slow flow [29]. However, we can note that the order of magnitude of the detachment coefficients we found is the same for the three runs, especially for models D2 and D3 (see Table 2).

As can be seen in Figs. 2–4, simulations with a detachment function based on discharge  $Q$  as proposed by Uehlinger et al. [16] or friction velocity do not reproduce the decrease of biomass after initial growth. In fact, simulation with the discharge gives faithful peak reproductions before stabilization around plateau, as can be clearly seen in Figs. 3 and 4. The same observations can be made in the three figures (2, 3, and 4), for simulations with  $u_*$  as external physical variable for forcing chronic detachment. Nevertheless, the values of the peaks reached with this formulation are closer to those measured than those obtained with the discharge  $Q$  as external physical variable for forcing chronic detachment.

Even if we can see in Fig. 3, a little decrease in biomass between the peak reached on day 20 and the stabilization that occurred from day 35, simulations with the third formulation (roughness Reynolds number  $k^+$ ) are the ones that reproduce well the decrease of periphytic biomass in the loss phase (Figs. 2–4).

Values of the correlation coefficient as can be seen in figures (2, 3, and 4) are greater with simulations

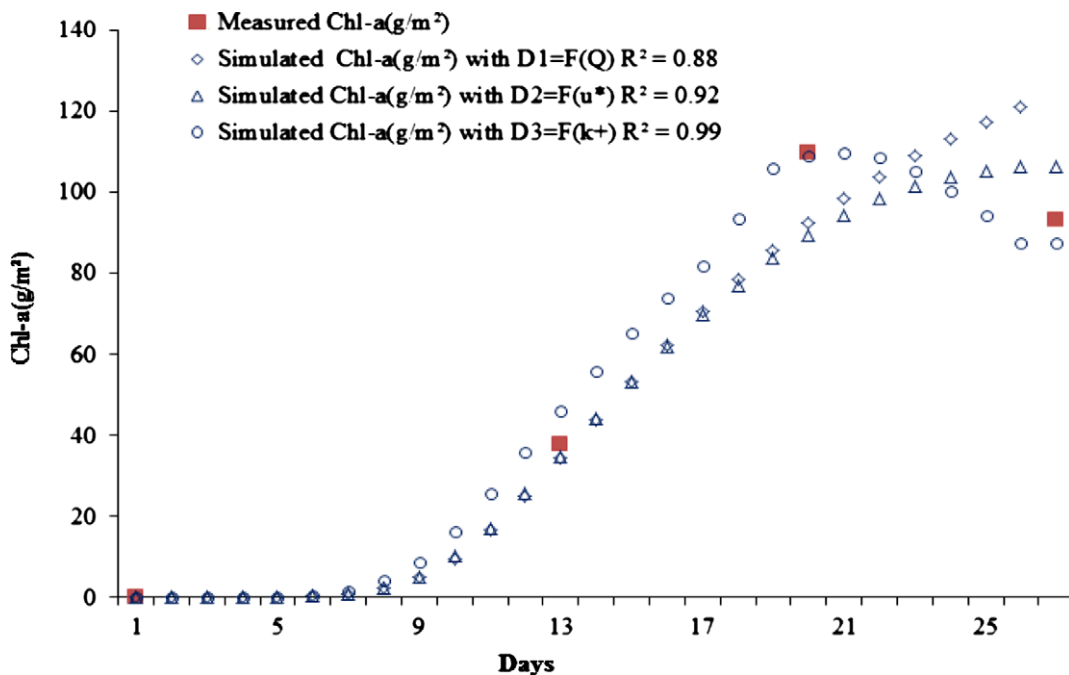


Fig. 2. Comparison of measured Chl-a ( $\text{g/m}^2$ ) and simulated values (Run1,  $Q=7.51/\text{s}$ ) with the three equations (D1, D2, and D3) for detachment:  $D1 = C_{det}QB$  ( $R^2=0.88$ ),  $D2 = C'_{det}u_*B$  ( $R^2=0.92$ ), and  $D3 = C''_{det}k^+B$  ( $R^2=0.99$ ).

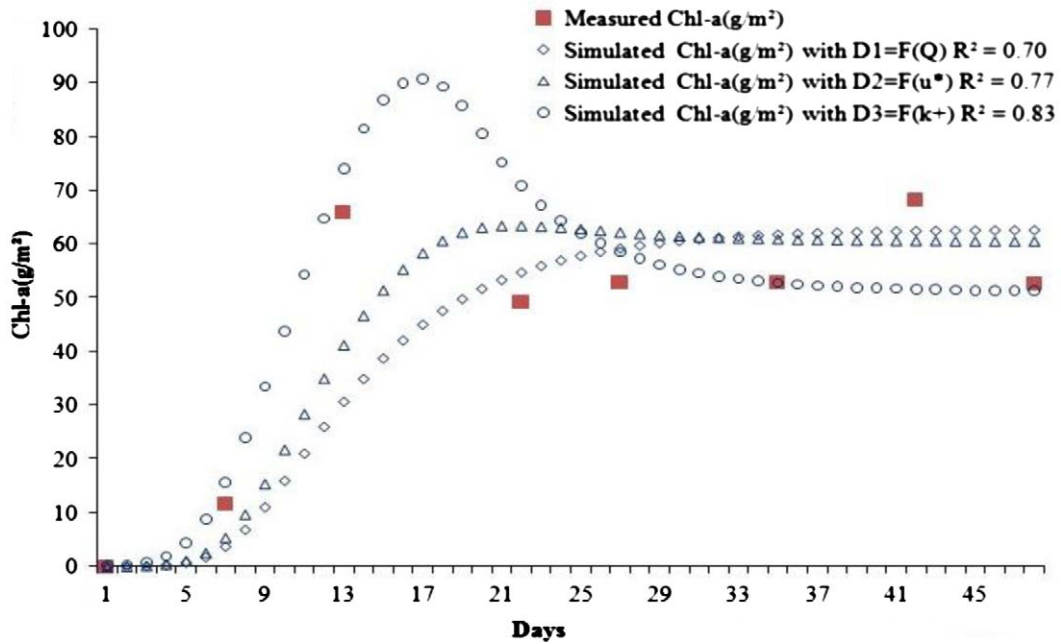


Fig. 3. Comparison of measured Chl-a ( $\text{g}/\text{m}^2$ ) and simulated values (Run2,  $Q=121/\text{s}$ ) with the three equations ( $D1$ ,  $D2$ , and  $D3$ ) for detachment:  $D1 = C_{\text{det}}QB$  ( $R^2=0.70$ ),  $D2 = C'_{\text{det}}u_*B$  ( $R^2=0.77$ ), and  $D3 = C''_{\text{det}}k^+B$  ( $R^2=0.83$ ).

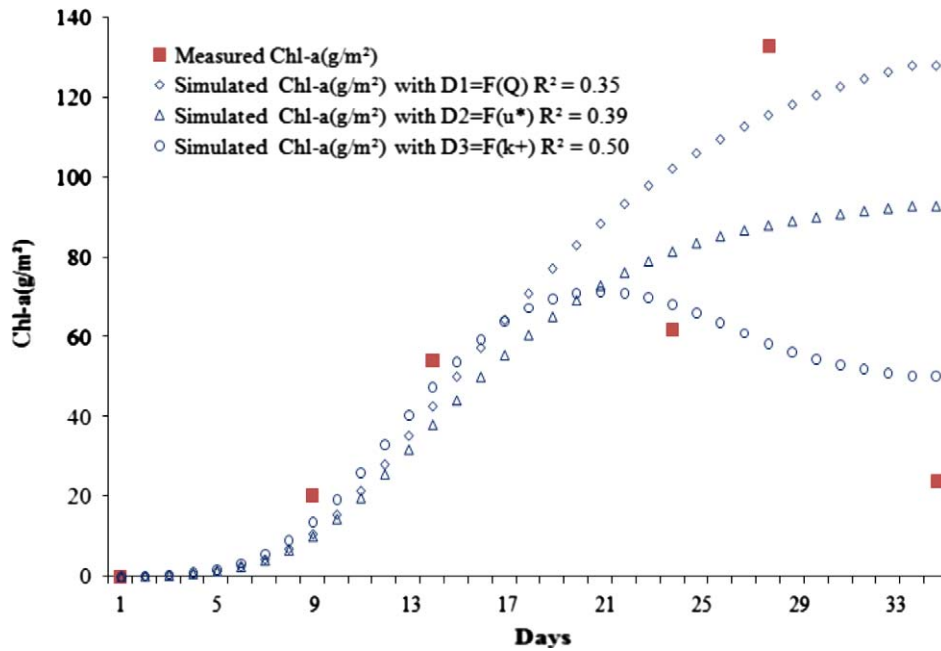


Fig. 4. Comparison of measured Chl-a ( $\text{g}/\text{m}^2$ ) and simulated values (Run3,  $Q=191/\text{s}$ ) with the three equations ( $D1$ ,  $D2$ , and  $D3$ ) for detachment:  $D1 = C_{\text{det}}QB$  ( $R^2=0.35$ ),  $D2 = C'_{\text{det}}u_*B$  ( $R^2=0.39$ ), and  $D3 = C''_{\text{det}}k^+B$  ( $R^2=0.50$ ).

using friction velocity  $u_*$  and greater yet using roughness Reynolds number  $k^+$  as external physical variables for forcing chronic detachment ( $R^2=0.99$  for Run1,  $R^2=0.83$  for Run2 and  $R^2=0.50$  for Run3).

Similarly, Graba et al. [33] using other experimental data concluded that the dynamics of epilithic matter and more generally, periphytic matter is better

simulated by taking the roughness Reynolds number  $k^+$  as the external variable of the detachment.

Values of the boundary layer parameters given in Table 1 show that the global tendency in Labiod et al. [28] experiments is that the periphytic biofilm induced an increase in the friction velocity  $u_*$ , the Nikuradse equivalent roughness height  $k_s$ , and then the roughness Reynolds Number  $k^+$ . Nevertheless, in Run2, the roughness knows a phase of smoothing with a decrease of friction velocity  $u_*$  and Roughness Reynolds Number  $k^+$  in the two first weeks (see Table 1). Whereas, in Graba et al. [33] experimental results, we observed a smoothing with a decrease in  $k_s$  as periphytic matter developed.

The main structural difference in the development of the roughness can be inferred from photographs taken in these two experimental studies. In Labiod et al. [28], the available space in the hollows between the PVC rods (diameter 10 mm) was negligible, so in the beginning of experiment, the periphytic matter covered all the surface of the rods in contact with the flow. This was followed by a development of long and flexible filaments and colonial algae that significantly increased the amount of surface area and completely changed the initial spatial wavelength prescribed by the PVC rods, inducing an important increase in shear stress, roughness height, and friction velocity [28].

In the case of Graba et al. [33], growth occurred between the artificial cobbles (20 mm high and 37 mm wide) and gradually filled the available space without any effect of nutrient depletion near the bottom. Thus the drag was declined by the presence of periphytic matter between the cobbles, leading to a decrease in shear stress, roughness height, and friction velocity [33].

Hence, the numerical investigations on chronic detachment of periphytic matter, using two contrasting transitions of roughness and friction velocity: smoothing in the case of Graba et al. [33], and increasing of friction velocity and roughness height in the case of Labiod et al. [28], show the same results. The roughness Reynolds number  $k^+$  seems to be the best external physical variable for forcing the chronic detachment process.

In fact, loss of periphytic matter was related not only to local flow conditions, but also to the shape and dimension of the substrate roughness and its variations depending on the amount of the biofilm matter present and its form, which was well described by the Nikuradse equivalent sand roughness  $k_s$ .

These results also agree with Douglas [43] who recognized that different sizes of stones supported different densities, dynamics, and species of periphytic

matter even for similar nutrient conditions, and that the biomass and species composition of periphytic communities are strongly influenced by substratum–current interactions [43]. Thus, the size of the substratum and its evolution are well described in the formulation we used by means of the equivalent sand roughness  $k_s$ , and the substratum–current interactions are described by roughness Reynolds number  $k^+$ .

These results are also confirmed by studies of flows over submerged canopies (aquatic vegetation) which conclude that the shear layer at the top of a submerged canopy generates coherent vortices that control the exchange between the canopy and the overflowing fluid [44,45]. Thus, the exchange phenomena that occur in the near-bed layer, e.g. vertical transport of nutrients and pollutants in submerged aquatic canopies [45], vertical flux over urban canopies [46,47], and chronic detachment of periphytic biofilm [33], are not related to a single turbulence descriptor such as the friction velocity  $u_*$ , but require at least two descriptors, the friction velocity  $u_*$  and the Nikuradse equivalent sand roughness  $k_s$  here in the case of chronic detachment of periphyton.

Many different formulations have been proposed in the literature to model the detachment process. Horner et al. [31] proposed a formulation with an empirical power law, while Saravia et al. [15] proposed a term with a square power law relating the detachment to an excess of kinetic energy. In the present study, we used a term proportional to  $k_s u_*$ , a form that is closely related to the concept of exchange velocity  $U_E$  introduced by Hamlyn and Britter [46] and Bentham and Britter [47] to describe vertical mass flux from the canopy layer to the external flow in turbulent boundary layers over roughness. Those authors showed experimentally and numerically that  $U_E$  is proportional to the friction velocity  $u_*$ , with a factor that depends on the difference in velocity between the canopy layer and the flow above, i.e. something indirectly related to the Nikuradse equivalent sand roughness height  $k_s$ . In other words, the chronic detachment can be seen as a permanent extraction by the hydrodynamics of some part of the biomass that, together with the hemispheres, forms the canopy sublayer.

## 5. Conclusions

The present investigation is a contribution to improve the periphyton chronic detachment process modeling. Thus, hydrodynamic and biological measurements from Labiod et al. [28] were used to test the relevance of three formulations for the chronic detachment term in simulating the dynamics of periphyton

growth with a simplified model adapted from Uehlinger et al. [16]. Comparisons of the results of numerical simulations with biological measurements revealed that chronic detachment was better simulated by taking the roughness Reynolds number as the external variable of detachment. In fact, loss of epilithic matter was related not only to local hydrodynamic conditions, but also to changes in bottom roughness, which depends on the amount of the periphyton matter present and its form, and which was well described by the Nikuradse equivalent sand roughness  $k_s$ .

These results support the improvement of Fothi [27] and Graba et al. [33] in modeling epilithic biomass dynamics with the equation of Uehlinger [16]. This, by substituting the flow discharge with friction velocity or roughness Reynolds number  $k^+$ , as external physical variable for forcing the chronic detachment process. This result sheds a new light on the role of the local hydrodynamics in the catastrophic detachment process associated with floods, and it suggests improving the term describing this process in the same way by considering local hydrodynamics variables rather than flow in the predictive equation of Uehlinger [16].

It is important to underline that turbulence not only controls the detachment process, but also has a strong influence on growth process and biochemical fluxes through the transfer rates of nutrients, or carbon dioxide and oxygen, from the outer layer to inside the periphytic matter. Thus, the influence of turbulence on growth processes could be incorporated into future refinements of the model allowing further consideration on the evolution of turbulence intensities and velocity profiles on the different layers in and above the periphytic biofilm (roughness layer, logarithmic layer, and outer layer).

## Notations

|   |   |
|---|---|
| $A$   | — log low roughness geometries constant   |
| $B$   | — biomass, $\text{g}/\text{m}^2$  |
| $B_{\text{init}}$   | — initial biomass, $\text{g}/\text{m}^2$  |
| $C$   | — colonization function, $\text{g m}^{-2} \text{days}^{-1}$   |
| $C_{\text{det}}$ , $C'_{\text{det}}$ and $C''_{\text{det}}$ | — empirical detachment coefficients, $\text{s}/\text{m}^3 \text{days}^{-1}$ , $\text{s}/\text{m days}^{-1}$ , and $\text{days}^{-1}$ , respectively |
| $\text{Chl-a}$  | — chlorophyll- <i>a</i> , $\text{g}/\text{m}^2$   |
| $D$   | — detachment function, $\text{g}/\text{m}^2 \text{days}^{-1}$   |
| $G$   | — growth function, $\text{g}/\text{m}^2 \text{days}^{-1}$   |
| $k_{\text{inv}}$  | — inverse half-saturation constant, $\text{g}^{-1} \text{m}^{-2}$   |
| $k_s$   | — Nikuradse equivalent sand roughness, cm   |
| $k^+$   | — roughness Reynolds number ( $=u_*k_s/\nu$ )   |

|                    |  |
|--------------------|--|
| $u_*$              | — friction velocity, $\text{cm}/\text{s}^1$ or $\text{m}/\text{s}$ |
| $\mu_{\text{max}}$ | — maximum specific growth, $\text{days}^{-1}$                      |
| $\nu$              | — water kinetic viscosity, $10^{-6} \text{m}^2 \text{s}^{-1}$      |

## References

- [1] B.J.F. Biggs, H.A. Thomsen, Disturbance of stream periphyton by perturbations in shear stress: Link to structural failure and differences in community resistance, *J. Phycol.* 31 (1995) 233–241.
- [2] B.J.F. Biggs, Patterns in benthic algae of streams, in: R.J. Stevenson, M.L. Bothwell, R.L. Lowe (Eds), *Algal Ecology: Freshwater Benthic Ecosystems*, Academic Press, San Diego, CA, pp. 31–56, 1996.
- [3] D. Hart, C. M. Finelli, Physical–biological coupling in streams: The pervasive effects of flow on benthic organisms, *Annu. Rev. Ecol. Syst.* 30 (1999) 363–395.
- [4] G.W. Minshall, Autotrophy in stream ecosystems, *Bioscience* 28 (1978) 767–771.
- [5] M.A. Lock, R.R. Wallace, J.W. Costerton, R.M. Ventullo, S.E. Charlton, River epilithon: Towards a structural-functional model, *Oikos* 42 (1984) 10–22.
- [6] R.L. Fuller, J.L. Roelofs, T.J. Frys, The importance of algae to stream invertebrates, *J. N. Am. Benthol. Soc.* 5 (1986) 290–296.
- [7] M.S. Mayer, G.E. Likens, The importance of algae in a shaded head water stream as a food of an abundant caddisfly (Trichoptera), *J. N. Am. Benthol. Soc.* 6 (1987) 262–269.
- [8] M.J. Winterbourn, Interactions among nutrients, algae and invertebrates in New Zealand mountain stream, *Freshwater Biol.* 23 (1990) 463–474.
- [9] B.J.F. Biggs, G.M. Price, A survey of filamentous algal proliferations in New Zealand rivers, *New Zeal. J. Mar. Fresh.* 21 (1987) 175–191.
- [10] D.F. Turner, G.J. Pelletier, B. Kasper, Dissolved oxygen and pH modeling of a periphyton dominated, nutrient enriched river, *J. Environ. Eng.* 135(8) (2009) 645–652.
- [11] M. Bessenasse, A. Kettab, A. Paquier, P. Ramez, G. Gale, Simulation numérique de la sédimentation dans les retenues de barrages: cas de la retenue de Zardezas, Algérie, *Rev. Sci. Eau* 16 (2003) 103–122.
- [12] R.J. Stevenson, Effects of currents and conditions simulating autogenically changing microhabitats on benthic diatom immigration, *Ecology* 64 (1983) 1514–1524.
- [13] M.A. Reiter, Interactions between the hydrodynamics of flowing water and development of a benthic algal community, *J. Fresh. Ecol.* 3(4) (1986) 511–517.
- [14] M. Hondzo, H. Wang, Effects of turbulence on growth and metabolism of periphyton in a laboratory flume, *Water Resour. Res.* 38(12) (2002) 1277, doi: 10.1029/2002WR001409.
- [15] L. Saravia, F. Momo, L.D. Boffi Lissin, Modelling periphyton dynamics in running water, *Ecol. Model.* 114(1) (1998) 35–47.
- [16] Ú. Uehlinger, H. Bührer, P. Reichert, Periphyton dynamics in a floodprone prealpine river: Evaluation of significant processes by modelling, *Freshwater Biol.* 36 (1996) 249–263.
- [17] S. Boulétreau, F. Garabetian, S. Sauvage, J.M. Sánchez-Pérez, Assessing the importance of self-generated detachment process in river biofilm models, *Freshwater Biol.* 51(5) (2006) 901–912, doi: 10.1111/j.1365-2427.2006.01541.x.
- [18] S. Boulétreau, O. Izagirre, F. Garabetian, S. Sauvage, A. Elo-segi, J.M. Sánchez-Pérez, Identification of a minimal adequate model to describe the biomass dynamics of river epilithon, *River. Res. Applic.* 24(1) (2008) 36–53, doi: 10.1002/rra.1046.
- [19] I. Nezu and H. Nakagawa, *Turbulence in open-channel flows*, Balkema, Rotterdam, 1993.
- [20] M.A. Reiter, Development of benthic algal assemblages subjected to differing near-substrate hydrodynamic regimes, *Can. J. Fish. Aquat. Sci.* 46 (1989a) 1375–1382.



- [21] M.A. Reiter, The effect of a developing algal assemblage on the hydrodynamics near substrates of different size, *Arch. Hydrobiol.* 115(2) (1989b) 221–244.
- [22] V. Nikora, D. Goring, B. Biggs, On stream periphyton–turbulence interactions, *New Zeal. J. Marine Freshwater Res.* 31(4) (1997) 435–448.
- [23] V. Nikora, D. Goring, B. Biggs, A simple model of stream periphyton–flow interactions, *Oikos* 81(3) (1998) 607–611.
- [24] B.J.F. Biggs, C.W. Hickey, Periphyton responses to a hydraulic gradient in a regulated river in New Zealand, *Freshwater Biol.* 32(1) (1994) 49–59.
- [25] R. Godillot, T. Ameziane, B. Caussade, J. Capblanc, Interplay between turbulence and periphyton in rough open-channel flow, *J. Hydraul. Res.* 39(3) (2001) 227–239.
- [26] V. Nikora, D. Goring, B. Biggs, Some observations of the effects of micro-organisms growing on the bed of an open channel on the turbulence properties, *J. Fluid Mech.* 450 (2002) 317–341.
- [27] A. Fothi, Effets induits de la turbulence benthique sur les mécanismes de croissance du périphyton, Ph.D. Thesis., 143 pp., INP de Toulouse, 2003.
- [28] C. Labiod, R. Godillot, B. Caussade, The relationship between stream periphyton. Dynamics and near-bed turbulence in rough open-channel flow, *Ecol. Model.* 209(2–4) (2007) 78–96, doi: 10.1016/j.ecolmodel.2007.06.011.
- [29] F.Y. Moulin, Y. Peltier, Y. Bercovitz, O. Eiff, A. Beer, C. Pen, S. Bouletreau, F. Garabétian, M. Sellali, J. Sanchez-Perez, S. Sauvage, D. Baque, Experimental study of the interaction between a turbulent flow and a river biofilm growing on macrorugosities, *Advances in hydro-science and engineering*, (VIII), ICHE-IAHR, Nagoya, Japan, 2008, pp. 1887–1896.
- [30] R.R. Horner, E.B. Welch, Stream periphyton development in relation to current velocity and nutrients, *Can. J. Fish. Aquat. Sci.* 38(4) (1981) 449–457.
- [31] R.R. Horner, E.B. Welch and R.B. Veenstra, Development of nuisance periphytic algae in laboratory streams in relation to enrichment and velocity, in: R.G. Wetzel (Ed.), *Periphyton of Freshwater Ecosystems*, W. Junk Publishers, The Hague, pp. 121–164, 1983.
- [32] R.J. Stevenson, An introduction to algal ecology in freshwater benthic habitats, in: R.J. Stevenson, M.L. Bothwell, Lowe RL. (Eds), *Algal Ecology: Freshwater Benthic Ecosystems*, Academic Press, San Diego, CA, pp. 3–30, 1996.
- [33] M. Graba, F.Y. Moulin, S. Bouletreau, F. Garabétian, A. Kettab, O. Eiff, J.M. Sanchez-Pérez, S. Sauvage, Effect of near-bed turbulence on chronic detachment of epilithic biofilm in artificial rough, open channel flow: Experimental and modeling approaches, *Water Resour. Res.* 46 (2010) W11531, doi: 10.1029/2009WR008679.
- [34] N. Flipo, S. Even, M. Poulin, M.H. Tusseau-Vuillemin, T. Ameziane, A. Dauta, Biogeochemical modelling at the river scale: Plankton and periphyton dynamics. Grand Morin case study, France, *Ecol. Model.* 176(3–4) (2004) 333–347, doi: 10.1016/j.ecolmodel.2004.01.012.
- [35] C. McIntire, Periphyton dynamics in laboratory streams: A simulation model and its implications, *Ecol. Monogr.* 34(3) (1973) 399–420.
- [36] F. Momo, A new model for periphyton growth in running waters, *Hydrobiologia* 299(3) (1995) 215–218.
- [37] T. Asaeda, D. Hong Son, Spatial structure and populations of a periphyton community: A model and verification, *Ecol. Model.* 133 (2000) 195–207.
- [38] T. Asaeda, D. Hong Son, A model of the development of a periphyton community resource and flow dynamics, *Ecol. Model.* 137 (2001) 61–75.
- [39] R. Belkhadir, B. Capdeville, H. Roques, Fundamental descriptive study and modelization of biological film growth:-I. Fundamental descriptive study of biological film growth, *Water Res.* 22(1) (1988) 59–69.
- [40] B. Capdeville, R. Belkhadir, H. Roques, Fundamental descriptive study and modelization of biological film growth:-I. A new concept of biological film growth modelization, *Water Res.* 22(1) (1988) 71–77.
- [41] M.T. Auer, R.P. Canale, Ecological studies and mathematical modelling of Cladophora in Lake Huron: 3. The dependence of growth rates on internal phosphorus pool size, *J. Great Lakes Res.* 8 (1982) 93–99.
- [42] M.A. Borchardt, Nutrients, in: R.J. Stevenson, M.L. Bothwell, Lowe RL. (Eds), *Algal Ecology: Freshwater Benthic Ecosystems*, Academic Press, San Diego, CA, pp. 183–227, 1996.
- [43] B. Douglas, The ecology of the attached diatoms and other algae in a small stony stream, *J. Ecol.* 45 (1958) 295–322.
- [44] A. Cattaneo, T. Kerimian, M. Roberge, J. Marty, Periphyton distribution and abundance on substrata of different size along a gradient of stream trophy, *Hydrobiologia* 354 (1997) 101–110.
- [45] H. Nepf, M. Ghisalberti, B. White, E. Murphy, Retention time and dispersion associated with submerged aquatic canopies, *Water Resour. Res.* 43(4) (2007) 55–66, doi: 10.1029/2006WR005362.
- [46] D. Hamlyn, R. Britter, A numerical study of the flow field and exchange processes within a canopy of urban-like roughness, *Atmos. Environ.* 39 (2005) 3243–3254.
- [47] T. Bentham, R. Britter, Spatially averaged flow over urban-like roughness, *Atmos. Environ.* 37 (2003) 115–125.